Decoherence and thermalization in a simple bosonic system

Pavel Cejnar,[1,2,*] Vladimir Zelevinsky,[3,†] and Valentin V. Sokolov[4,‡]
[1]*Institute of Particle and Nuclear Physics, Charles University, V Holešovičkách 2, 180 00 Prague, Czech Republic*
[2]*Institute of Theoretical Physics, University of Stellenbosch, 7602 Matieland, South Africa*
[3]*National Superconducting Cyclotron Laboratory, Michigan State University, East Lansing, Michigan 48824-1321*
[4]*Budker Institute of Nuclear Physics, 630090 Novosibirsk, Russia*
(Received 23 October 2000; published 27 February 2001)

Properties of a parameter-dependent quantum system with the Hamiltonian $\hat{H}(\lambda)$ randomized by fluctuations of the parameter λ in a narrow range are investigated. The model employed (the interacting boson model-1) exhibits a crossover behavior at a critical parameter value. Due to the fluctuations, individual eigenstates $|\psi^{\alpha}(\lambda)\rangle$ of the Hamiltonian become statistical ensembles of states [density matrices $\hat{\varrho}^{\alpha}(\lambda)$], which allows us to study effects related to the decoherence and thermalization. In the decoherence part, we evaluate von Neumann and information entropies of the density matrices $\hat{\varrho}^{\alpha}(\lambda)$ and the overlaps of the eigenstates of the density matrix with various physically relevant bases. An increased decoherence at the '' phase transitional'' point and an exceptional role of the dynamic-symmetry U(5) basis are discovered. In the part devoted to the thermalization, we develop a method of how a given density matrix $\hat{\varrho}^{\alpha}(\lambda)$ can be represented by an equivalent canonical (thermal) ensemble. Thermodynamic consequences of the quantum ''phase transition'' (related, in particular, to the specific heat of the thermal equivalent) are discussed.

DOI: 10.1103/PhysRevE.63.036127 PACS number(s): 05.30.Ch, 05.70.Fh, 03.65.Yz

I. INTRODUCTION

In recent years, one can observe an increasing interest in physical models whose Hamiltonians contain random variables (see, e.g., Refs. [1–9]). The reasons why random Hamiltonians are found important in various areas of physics are very different. The randomness can, for instance, mimic the sampling of a multidimensional parameter space of a deterministic and stationary quantum-mechanical problem in question (especially if the actual Hamiltonian parameters are not precisely known, like in the case of nuclear interactions [3,5]). A great success of random matrix theory, in particular in applications of invariant ensembles of Hamiltonians (Gaussian orthogonal/unitary ensembles or the embedded ensembles) [2,3,9], is related to the fact that the averaging over random Hamiltonians of certain symmetry reveals the most generic dynamic properties. In contrast, the randomness can also represent real adiabatic fluctuations of an effective Hamiltonian in time [1] (like in the case of atoms subject to randomly varying external fields). In view of the very different purposes for studying random Hamiltonians, it does not surprise that the spectrum of relevant theoretical problems is very wide. Along with the problems well accommodated in physics, as the description of local correlations in spectra and eigenstates of complex systems, it extends to fundamental but still not fully understood problems related to the decoherence [6,10–12] and thermalization [4,13–16]. These aspects are addressed in the present paper.

The random Hamiltonian we use arises from a deterministic, parameter-dependent Hamiltonian $\hat{H}(\lambda)$ through fluctuations of the parameter λ in a narrow range, i.e.,

$$\hat{H}(\lambda) \rightarrow \hat{H}(\lambda + \delta\lambda), \tag{1}$$

where $\delta\lambda$ is a random variable. The concrete model employed, representing a simplified system of bosons, is described in Sec. II. The randomization in Eq. (1) implies that instead of definite energy eigenstates one has to deal with statistical ensembles of states (density matrices) and the corresponding energy distributions. Such a transition from pure to mixed states resembles the environment-induced decoherence process [10], widely discussed in connection with the fundamentals of quantum theory. One of the aims of this paper is to show that the study of random Hamiltonians of the type (1) can be instructive for understanding of decoherence effects that occur in realistic systems. A particularly interesting question concerns the relation of the formally introduced pointer basis [11,12], i.e., the eigenbasis of the density matrix, to the physically relevant bases. These problems are investigated in Sec. III. We find the evidence of a nontrivial and sensitive dependence of the pointer basis on specific properties of the unperturbed Hamiltonian.

Another part of the paper is devoted to the problem of thermalization in finite quantum systems [13]. It appears to hold generically that any system of particles with a sufficiently complex interaction can be, to a large extent, characterized by purely thermal attributes, like the grand canonical population of single-particle states or thermodynamic entropy in its relation to the complexity of the eigenstates [4,14–16]. Using the random Hamiltonian (1), we analyze in Sec. IV another method of assigning a temperature scale to a given system. A special attention is paid to the correspondence between thermal and quantum-mechanical properties of the system in the vicinity of the phase-transitional behavior [17].

*Electronic address: pavel.cejnar@mff.cuni.cz
†Electronic address: zelevinsky@nscl.msu.edu
‡Electronic address: v.v.sokolov@inp.nsk.su

II. THE MODEL

In the present work, the parameter-dependent Hamiltonian $\hat{H}(\lambda)$ of Eq. (1) was chosen within the framework of the interacting boson model (IBM), well known in the description of collective excitations of atomic nuclei [18,19]. In its simplest form (IBM-1), the model describes a system of a fixed total number N of bosons with spins 0 or 2 (s and d bosons). The model Hilbert space is finite, its basis being generated by N successive applications of boson creation operators $s^\dagger$ and/or $d^\dagger_\mu$ (where $\mu=-2,\ldots,+2$ is the spin projection) on a vacuum state $|0\rangle$. The most general IBM-1 Hamiltonian contains all possible one- and two-body terms and has five free parameters (if not counting the additive and scaling constants). Varying these parameters, one can reach the domains of the parameter space where the model possesses one of its possible dynamical symmetries; the Hamiltonian then becomes analytically solvable and integrable.

We use a simplified, single-parameter Hamiltonian that continuously covers the limiting cases of the SU(3) and U(5) dynamical symmetries

$$\hat{H}(\lambda)=\lambda\,\hat{n}_{\rm d}-\frac{1-\lambda}{N}\hat{Q}\cdot\hat{Q}. \tag{2}$$

Here

$$\hat{n}_d=d^\dagger\cdot\tilde{d} \tag{3}$$

is the d-boson number operator and

$$\hat{Q}_\mu=d^\dagger_\mu s+s^\dagger\tilde{d}_\mu-\frac{\sqrt{7}}{2}(d^\dagger\times\tilde{d})^{(2)}_\mu \tag{4}$$

is a quadrupole operator [''$\cdot$'' and '' $\times$'' stand for the scalar and tensor products, respectively, and $\tilde{d}_\mu=(-)^\mu d_{-\mu}$; the angular momentum in the IBM is defined as $\hat{L}_\mu=\sqrt{10}(d^\dagger\times\tilde{d})^{(1)}_\mu$]. The SU(3) dynamical symmetry is reached for $\lambda=0$ and the U(5) symmetry for $\lambda=1$; we therefore consider the parameter range $\lambda\in[0,1]$.

It is well known that the SU(3)$\rightarrow$U(5) transition has a critical character in the IBM [18,20,21]. For the Hamiltonian (2), a kind of a phase transition takes place at $\lambda\approx0.8$, where a multiple avoided crossing of levels in the lower part of the spectrum increases the efficiency of mixing of the corresponding eigenfunctions [17]. The form of the eigenstates changes drastically in this region resulting in an abrupt onset of the U(5) regime (similar to first-order phase transitions [22]). To be exact, for finite boson numbers one can only talk about quasicriticality because the transition is not truly discontinuous. It was shown, nevertheless, to be fast enough even for not too large boson numbers [17]. The λ-dependent energy spectrum $\{E^\alpha(\lambda)\}_{\alpha=1}^n$ of the states with angular momentum $L=0$ is shown in Fig. 1 for the total number of bosons $N=30$ (cf. Figs. 4 and 5 in Ref. [17]). In this case, the dimension $n=91$. A ''macroscopic'' avoided crossing of the levels located in the lower part of the spectrum can be identified in the critical $\lambda\approx0.8$ region, while some minor binary level collisions appear at other places. These structures will be shown to play an important role in the following analyses.

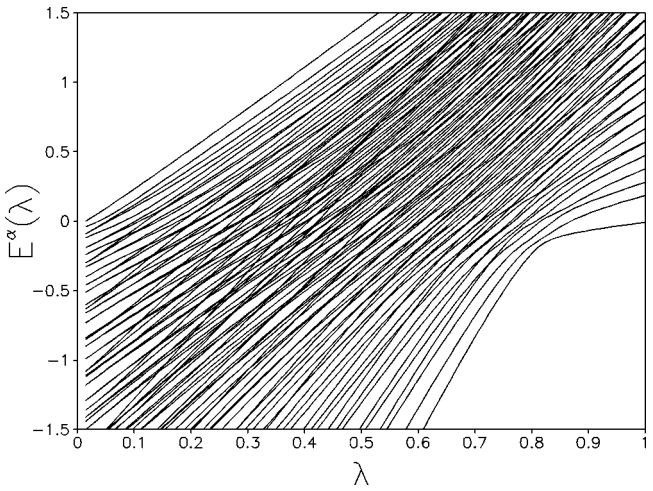

FIG. 1. The parameter-dependent $L=0$ spectrum of the Hamiltonian (2) with $N=30$.

After the randomization according to Eq. (1), the Hamiltonian can be expressed as

$$\hat{H}(\lambda+\delta\lambda)=\hat{H}(\lambda)+\delta\lambda\,\hat{H}' \tag{5}$$

with

$$\hat{H}'=\hat{n}_d+\frac{1}{N}\hat{Q}\cdot\hat{Q}. \tag{6}$$

We consider $\delta\lambda$ to be a Gaussian random variable with zero mean and dispersion $\sigma^2\ll1$. The unperturbed part of the Hamiltonian (5) is deterministic and carries the dependence of the problem on λ, while the randomness is introduced through the fluctuating strength of the perturbation $\hat{H}'$. Note that the incompatibility of both the terms in Eq. (5) (and thus the efficiency of the random perturbation) has no *a priori* parametric dependence since the commutator

$$[\hat{H}(\lambda),\hat{H}']=\frac{1}{N}[\hat{n}_d,\hat{Q}\cdot\hat{Q}]\neq0 \tag{7}$$

is independent of λ.

III. DECOHERENCE

Due to the fluctuations of the parameter λ in the Hamiltonian $\hat{H}(\lambda)$, any of its eigenstates $|\psi^\alpha(\lambda)\rangle=\Sigma_i a_i^\alpha(\lambda)|i\rangle$ transforms into a density operator defined [6] by

$$\hat{\varrho}^\alpha(\lambda)=\int d[\delta\lambda]\,|\psi^\alpha(\lambda+\delta\lambda)\rangle p(\delta\lambda)\langle\psi^\alpha(\lambda+\delta\lambda)|, \tag{8}$$

where $p(\delta\lambda)$ is the distribution of the fluctuations $\delta\lambda$ in Eq. (1). Equation (8) enables one to use the standard formalism of quantum statistical physics, calculating the ensemble av-

erage of any physical quantity A as $\langle A\rangle = \mathrm{tr}(\hat{A}\hat{\varrho})$. The ensemble averaging can be considered equivalent to the time averaging in case of slow, adiabatic fluctuations $\delta\lambda(t)$. In an arbitrary basis $\mathcal{B}\equiv\{|i\rangle\}_{i=1}^{n}$, the density operator (8) has the following form:

$$\langle i|\hat{\varrho}^{\alpha}(\lambda)|j\rangle \equiv \varrho_{ij}^{\alpha}(\lambda)_{\mathcal{B}} = \int d[\delta\lambda]p(\delta\lambda)a_j^{\alpha}(\lambda+\delta\lambda)^* a_i^{\alpha}(\lambda+\delta\lambda). \tag{9}$$

Its diagonalization then yields, at each point λ, the density-matrix eigenvalues $\rho_p^{\alpha}(\lambda)$ and eigenvectors $|\phi_p^{\alpha}(\lambda)\rangle$

$$\hat{\varrho}^{\alpha}(\lambda) = \sum_{p=1}^{n} |\phi_p^{\alpha}(\lambda)\rangle \rho_p^{\alpha}(\lambda) \langle \phi_p^{\alpha}(\lambda)|. \tag{10}$$

It is clear that the diagonalized form of the density matrix contains only information on the occupation probabilities of the density-matrix eigenstates and no quantum correlations. The eigenbasis

$$\mathcal{B}_{\mathrm{p}}^{\alpha}(\lambda) = \{|\phi_p^{\alpha}(\lambda)\rangle\}_{p=1}^{n} \tag{11}$$

will hereafter be called the *pointer basis*, in agreement with Refs. [10–12]. In our case it is associated with a given value of λ and the αth energy eigenstate. It should be stressed that whereas the pointer basis fundamentally results from an interaction of the given system with an environment (this makes initial pure states of the system develop into statistical mixtures) [10], in our case it arises through the fluctuation of λ.

The degree of ''impurity'' of a given mixed state $\hat{\varrho}$ is quantified [6] by von Neumann entropy $S=-\mathrm{tr}(\hat{\varrho}\ln\hat{\varrho})$, i.e., for the density matrix (10),

$$S^{\alpha}(\lambda) = -\sum_{p=1}^{n} \rho_p^{\alpha}(\lambda)\ln\rho_p^{\alpha}(\lambda). \tag{12}$$

It varies from zero for a pure state ($\rho_p=\delta_{pp_0}$) to $\ln n$ for a maximally uncertain mixed state ($\rho_p=1/n$). In a similar fashion, the degree of fragmentation in a fixed basis $\mathcal{B}$ can be expressed via Shannon information entropy (cf. Refs. [14,15,23–25] and references therein)

$$I_{\mathcal{B}}^{\alpha}(\lambda) = -\sum_{i=1}^{n} \varrho_{ii}^{\alpha}(\lambda)_{\mathcal{B}} \ln \varrho_{ii}^{\alpha}(\lambda)_{\mathcal{B}}. \tag{13}$$

Again, information entropy increases from 0 to $\ln n$ as the state is getting more fragmented in the basis $\mathcal{B}$. Von Neumann entropy (12) depends on both on-diagonal and off-diagonal matrix elements of the density matrix in any basis and its value is basis independent. On the contrary, information entropy (13) neglects correlations carried by the off-diagonal elements in the specific basis $\mathcal{B}$ and thus depends on $\mathcal{B}$. It would coincide with von Neumann entropy if the correlations vanish due to a dynamical decoherence process induced by an interaction with additional degrees of freedom. In case of no extra interaction, however, information entropy merely disregards a part of quantum knowledge available on the system. [See, however, the discussion [14,15] of the inter-relation between thermal (von Neumann) invariant entropy, wave function (information) entropy, and single-particle fermion entropy calculated in the nuclear shell model basis; for the self-consistent mean field they are practically equivalent due to the self-averaging.] For the purpose of this paper, we call von Neumann entropy (12) *coherent* (similar to ''correlational'' of Ref. [6]), whereas information entropy (13) will be referred to as *incoherent*.

The family of physically informative entropies can be supplemented by *overlap* entropy O. We define it as a measure of the average overlap between the two bases, $\mathcal{B}\equiv\{|i\rangle\}_{i=1}^{n}$ and $\mathcal{B}'\equiv\{|j'\rangle\}_{j=1}^{n}$

$$O(\mathcal{B},\mathcal{B}') = -\frac{1}{n}\sum_{i=1}^{n}\sum_{j=1}^{n} |\langle i|j'\rangle|^2 \ln|\langle i|j'\rangle|^2. \tag{14}$$

Its minimal value, $O=0$, is reached for $\mathcal{B}=\mathcal{B}'$. As the two bases deviate from each other, the overlap entropy increases but—because of the orthogonality constraints—it can never reach the uppermost limit $\ln n$. A probable saturation value is close to $O_{\mathrm{ran}}\approx\ln(0.48n)$, which is the asymptotic expectation value of the overlap entropy for two randomly chosen bases, as determined by the random-matrix theory. Information entropy of eigenfunctions studied from the viewpoint of many-body chaos [15,25] is in fact overlap entropy of the eigenbasis and a ''simple'' reference basis, for example, the mean field one.

Of special interest in the present problem is the choice when the reference basis $\mathcal{B}$ of incoherent entropy (13) coincides with the local eigenbasis of $\hat{H}(\lambda)$,

$$\mathcal{B}_{\mathrm{l}}(\lambda) \equiv \{|\psi^{\beta}(\lambda)\rangle\}_{\beta=1}^{n}. \tag{15}$$

Perturbation theory can be used to develop a simple formula relating coherent and incoherent entropy with overlap entropy between the local and pointer bases. Namely, if $\delta\lambda$ in Eq. (5) is considered to be small enough, it is sufficient to expand the density matrix (9) in the local basis (15) up to the $\langle\delta\lambda^2\rangle\equiv\sigma^2$ terms [6]. In this approximation, the density matrix $\hat{\varrho}^{\alpha}$ corresponding to the energy term $E^{\alpha}(\lambda)$ has just two nonzero eigenvalues, $p=1$ and 2,

$$\rho_1^{\alpha}(\lambda) \approx 1-\sigma^2 w^{\alpha}(\lambda), \tag{16}$$

$$\rho_2^{\alpha}(\lambda) \approx \sigma^2 w^{\alpha}(\lambda), \tag{17}$$

where

$$w^{\alpha}(\lambda) = \sum_{\beta\neq\alpha} [v_{\beta}^{\alpha}(\lambda)]^2, \tag{18}$$

$$v_{\beta}^{\alpha}(\lambda) = \frac{\langle\psi^{\beta}(\lambda)|\hat{H}'|\psi^{\alpha}(\lambda)\rangle}{E^{\beta}(\lambda)-E^{\alpha}(\lambda)}, \tag{19}$$

with the corresponding eigenvectors

$$|\phi_1^\alpha(\lambda)\rangle \approx |\psi^\alpha(\lambda)\rangle, \tag{20}$$

$$|\phi_2^\alpha(\lambda)\rangle \approx \frac{1}{\sqrt{w^\alpha(\lambda)}} \sum_{\beta\neq\alpha} v_\beta^\alpha(\lambda)|\psi^\beta(\lambda)\rangle. \tag{21}$$

For coherent and incoherent entropy in Eqs. (12) and (13), we obtain

$$S^\alpha(\lambda) \approx -\rho_1^\alpha(\lambda)\ln\rho_1^\alpha(\lambda) - \rho_2^\alpha(\lambda)\ln\rho_2^\alpha(\lambda) \tag{22}$$

and

$$I^\alpha_{\mathcal{B}_l(\lambda)}(\lambda) \approx -\rho_1^\alpha(\lambda)\ln\rho_1^\alpha(\lambda) - \sum_{\beta\neq\alpha}[\sigma v_\beta^\alpha(\lambda)]^2 \ln[\sigma v_\beta^\alpha(\lambda)]^2, \tag{23}$$

respectively, while overlap entropy between the local and pointer bases is given by

$$O[\mathcal{B}_l(\lambda), \mathcal{B}_p^\alpha(\lambda)] \approx -\frac{1}{n}\sum_{\beta\neq\alpha}\frac{[v_\beta^\alpha(\lambda)]^2}{w^\alpha(\lambda)}\ln\frac{[v_\beta^\alpha(\lambda)]^2}{w^\alpha(\lambda)}. \tag{24}$$

Whereas coherent and incoherent entropy, Eqs. (22) and (23), respectively, both vanish if $\sigma^2\to 0$, the overlap entropy in Eq. (24) stays nonzero for any $\sigma^2>0$ because even a small perturbation singles out the same direction in density-matrix eigenspace [6] regardless of the strength, see Eq. (21). Combining the last expression with Eqs. (22) and (23), one obtains

$$I^\alpha_{\mathcal{B}_l(\lambda)}(\lambda) - S^\alpha(\lambda) \approx \sigma^2 n\, w^\alpha(\lambda) O[\mathcal{B}_l(\lambda), \mathcal{B}_p^\alpha(\lambda)]. \tag{25}$$

This means that incoherent entropy in the local basis is larger than corresponding coherent entropy, the difference being proportional to overlap entropy between the local and pointer bases. In general, the difference of incoherent entropy, Eq. (13), in an arbitrary basis $\mathcal{B}\equiv\{|i\rangle\}_{i=1}^n$ and coherent entropy, Eq. (12), is not negative and can be written down as

$$I_\mathcal{B} - S = \sum_{p=1}^n \rho_p\left[\ln\rho_p - \sum_{i=1}^n |\langle i|\phi_p\rangle|^2 \ln\left(\sum_{p'=1}^n \rho_{p'}|\langle i|\phi_{p'}\rangle|^2\right)\right] \tag{26}$$

(we skipped here the reference to α and λ). Thus, for a pure state $\rho_p=\delta_{pp_0}$, $S=0$ while $I_\mathcal{B}$ gives information entropy of the pointer state $|\phi_{p_0}\rangle$ in the basis $\mathcal{B}$. Only in the chaotic limit of $\rho_p=1/n$, we come to $S=I_\mathcal{B}=\ln n$.

The above discussed entropies were calculated numerically for the random Hamiltonian (5) with $N=30$. The results for $L=0$ states labeled by $\alpha=1$, 4, and 30 (cf. Fig. 1) are shown in Figs. 2, 3, and 4, respectively. The Gaussian distribution $p(\delta\lambda)$ was used with $\langle\delta\lambda\rangle=0$ and $\sqrt{\langle\delta\lambda^2\rangle}=\sigma=0.01$, and the parameter range displayed is $\lambda\in[0.03,0.97]$. The upper panels of Figs. 2–4 present coherent entropy (12) and incoherent entropy (13) in the local basis $\mathcal{B}=\mathcal{B}_l(\lambda)$. The used value of σ is clearly small enough

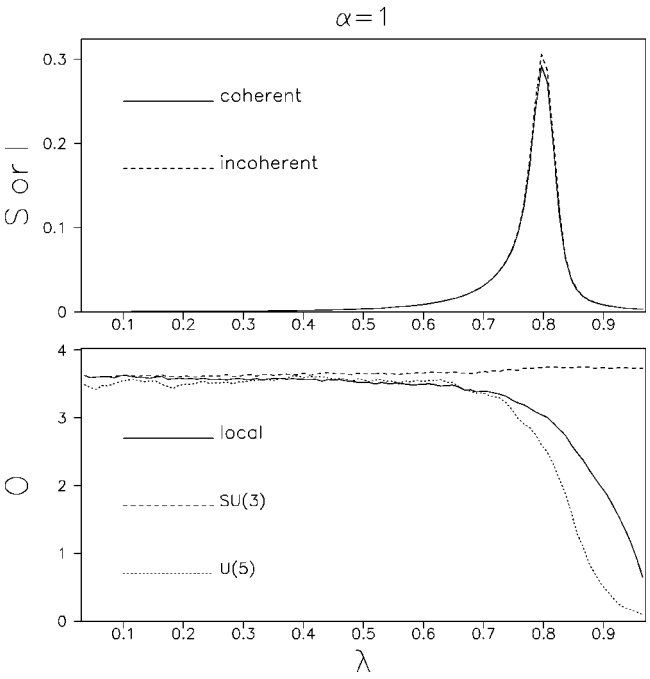

FIG. 2. Entropies characterizing the density matrix (8) connected with the first $L=0$ eigenstate of the Hamiltonian (2) for $N=30$ bosons as functions of λ. The rms of the zero-mean Gaussian variable $\delta\lambda$ is $\sigma=0.01$. The coherent entropy and incoherent entropy in the local basis, Eqs. (12), (13), and (15), are drawn in the upper panel. The lower panel shows overlap entropies, Eq. (14), of the pointer basis with the local SU(3) and U(5) bases.

to keep the perturbative relation (25) valid. The respective lower panels display overlap entropies (14) of the pointer basis $\mathcal{B}_p^\alpha(\lambda)$ with the local basis $\mathcal{B}_l(\lambda)$, with the SU(3) basis $\mathcal{B}_l(\lambda=0)$, and with the U(5) basis $\mathcal{B}_l(\lambda=1)$. As seen from

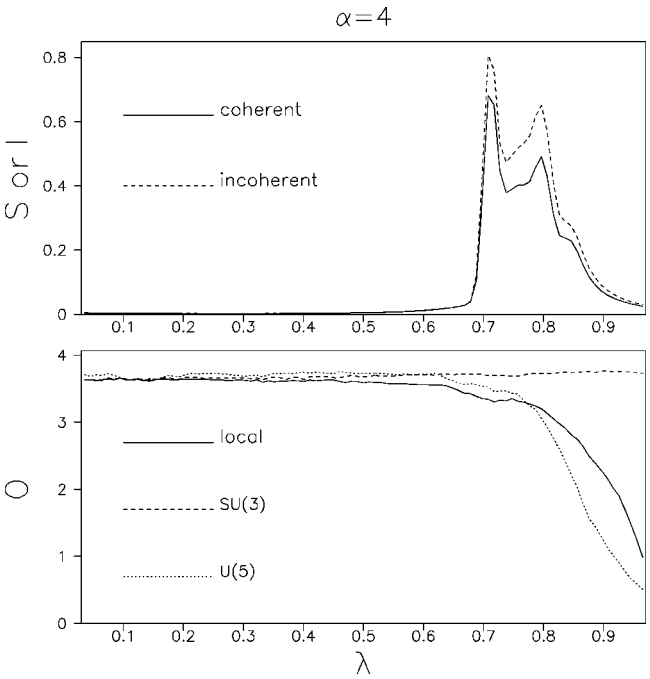

FIG. 3. The same as in Fig. 2, but for the fourth $L=0$ state.

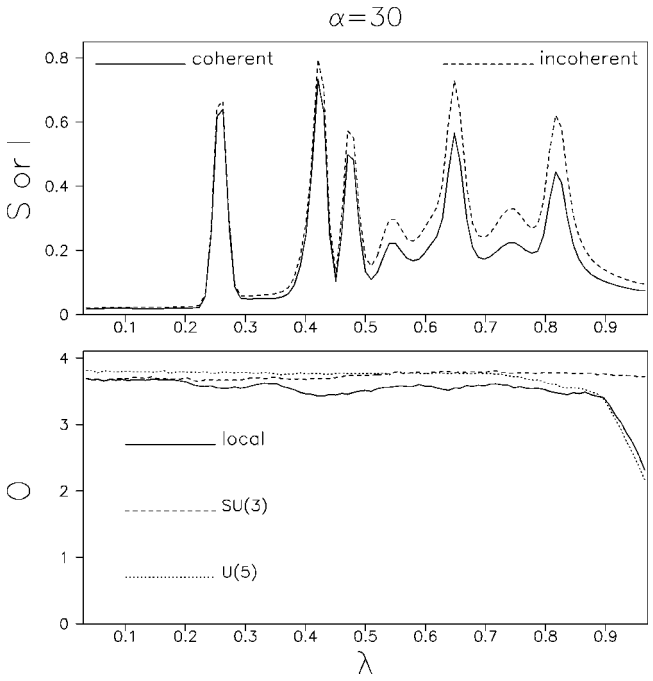

FIG. 4. The same as in Fig. 2, but for the thirtieth $L=0$ state.

the upper panels of Figs. 2–4, the response of the λ dependence of coherent and incoherent entropy varies substantially for different energy terms α. While the ensemble originating from the ground state ($\alpha=1$) produces a single peak of both coherent and incoherent entropy at the phase-transitional point $\lambda=0.8$, the other two ensembles lead to more complicated structures. In the case of $\alpha=4$ (Fig. 3), the increase of S and I still takes place in the phase-transitional region $0.7<\lambda<0.9$, but it does not have a single-peaked form. For $\alpha=30$ (Fig. 4), both S and I develop a chain of peaks ranging from $\lambda\approx 0.2$ to 0.9. The underlying mechanism responsible for these differences is the mixing of various eigenfunctions induced by the change of λ. It was extensively discussed in the framework of the universal decorrelation theory of parameter-dependent systems (see, e.g., Refs. [26,27]), and also specifically for the IBM-1 [17]. The proximity of levels enhances the efficiency of mixing [cf. Eq. (19)]. Indeed, under a scrutiny, one can find a one-to-one correspondence between the peaks of S and I in Figs. 3 and 4 and the avoided crossings of the respective lines ($\alpha=4$ and 30) with their neighbors in Fig. 1.

Overlap entropies in the lower panels of Figs. 2–4 also carry interesting physical information. First, the overlap between the pointer and SU(3) bases is essentially random within the whole parameter range displayed and for all three states considered (in the present case, the above-mentioned saturation value of overlap entropy is $O_{\mathrm{ran}}\approx 3.78$). On the other hand, inspite of the independence of the commutator in Eq. (7) on λ, the overlap of the pointer basis with the local and U(5) bases substantially increases (the overlap entropy decreases) above $\lambda\approx 0.8$; below this point it again reaches the random limit. Especially interesting is the fact that for $\alpha=1$ and 4 (Figs. 2 and 3), the pointer basis overlaps more with the U(5) basis than with the local bases for $\lambda\in[0.8,1]$. In this region, the U(5) basis serves as an ''attractor''—the pointer basis always deviates from the local basis in the direction of the U(5) basis. This finding seems to generalize the known sharp onset of the U(5) component in wave functions of low-lying states at the phase-transitional point [17]. It does not therefore surprise that—similar to the wave-function case—the preference of the U(5) basis to the local bases disappears for higher-energy states, like the one with $\alpha=30$ in Fig. 4.

We would like to emphasize here the relation of topics studied in this section to the general decoherence problem as discussed, for instance, in Refs. [10–12]. Our fluctuation scheme in Eq. (1) should describe the time-averaged properties of the system interacting with an external source of the noise (to describe in general the correspondence between random Hamiltonians—stationary or nonstationary—and problems containing unobserved degrees of freedom is an interesting but complicated task). In this connection, an important message of the above calculations is that the rate of decoherence, measured by the entropy production, may change drastically with the intrinsic state of the system embodied in our case in the value of the initial parameter λ in the Hamiltonian. This rate is maximal at the avoided-crossing places, particularly in the phase-transitional region. The pointer basis selected in the decoherence process also was shown to depend sensitively on the initial λ. Even for a small range of fluctuations $\delta\lambda$, the pointer basis can be completely different from the initial (local) basis of the system. This does not contradict the recent result [12] that the pointer basis tends to coincide with the energy eigenbasis in the weak system-environment coupling regime. In fact, the range of fluctuations is unrelated to the coupling strength; all the above calculations most likely correspond to the strong-coupling limit because the system can be seen as driven by the environment to undergo the parameter fluctuations.

IV. THERMALIZATION

Thermal properties of closed quantum systems are currently subject to intense discussions; see, for instance, Refs. [4,13–16] and the works cited there. In nuclear physics the language of statistical thermodynamics is exclusively used for the description of highly excited states. It appears that a typical wave function of a sufficiently complex (chaotic?) many-body system in a given range $E\pm\Delta E/2$ of excitation energy exhibits average properties expected for a thermally equilibrated system. Temperature T can be defined in terms of the smoothened density $\Omega(E,\ldots)$ of states of the closed system at given energy E (dots symbolize quantum numbers connected with other integrals of motion as angular momentum or parity) through the known formula

$$\frac{1}{T_{\mathrm{LD}}}\equiv\frac{\partial}{\partial E}\ln\Omega(E,\ldots). \tag{27}$$

The subscript '' LD'' here indicates the relation of this definition to the level density. Equation (27) can be understood with the aid of the argument that information entropy of eigenstates (in terms of some mean-field basis [14,15]) in-

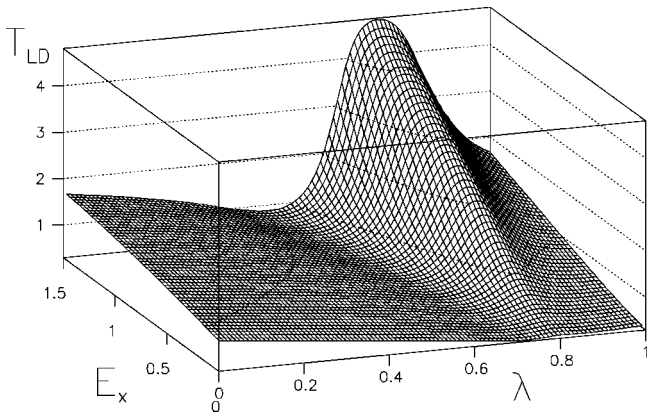

FIG. 5. Temperature from Eq. (27) given by the density of $L=0$ eigenstates of Eq. (2), $N=30$. The dependence on λ and on the excitation energy $E_x<1.5$ is shown.

creases with an increasing local density of states. In realistic systems, where $\Omega(E,\ldots)$ typically grows exponentially with energy, the equivalent temperature in Eq. (27) is always positive and also grows with E. For model systems with finite Hilbert space, however, the level density has a peaked form (most likely Gaussian) with the maximum at some energy E_0. The corresponding temperature is thus singular at $E=E_0$ and negative for $E>E_0$ (see Fig. 53 in Ref. [15]).

Temperature extracted according to Eq. (27) from the $L=0$ eigenspectrum of the Hamiltonian (2) with $N=30$ is shown in Fig. 5 as a function of the parameter λ and excitation energy E_x (counted from that of the ground state; see Fig. 1). The level density $\Omega(E)$ for this class of states was obtained by the Gaussian smoothening $\Omega(E)=\int G(E-E')\Omega'(E')dE'$ of the exact microscopic state density $\Omega'(E)=\Sigma_\alpha\delta[E-E^\alpha(\lambda)]$. Note that the energy range $E_x<1.5$ displayed in Fig. 5 contains a number of levels varying with λ (see Fig. 1). To ensure a smooth appearance of the function in Fig. 5, the width of the Gaussian $G(E-E')$ in the above convolution was chosen separately for each parameter value. The most interesting feature of Fig. 5 is the ridge at $\lambda\approx 0.8$. This corresponds to the phase-transitional region, where the spectrum as a whole is maximally compressed, but also maximally homogeneous, see Fig. 1. On the other hand, the valley with the lowest temperature on the left-hand side of the ridge in Fig. 5 coincides with the region of the maximal increase of the state density with energy (this becomes apparent if the spectrum in Fig. 1 is redrawn with a constant ground-state energy; see Fig. 4 in Ref. [17]).

Below we investigate another aspect of the thermalization problem. We mentioned that the tentative thermal properties of closed quantum systems can be discussed [4,14,15] as originating from features of individual eigenstates. However, the randomness in the Hamiltonian (1) enables one to use an alternative thermalization scheme [6] with the temperature assigned to the system directly via the statistical ensemble (8). For a given density operator $\hat{\varrho}^\alpha(\lambda)$, one can determine a corresponding canonical ensemble (the '' thermal equivalent'') with the same basic physical features. The problem can be formulated in a general way: given a density matrix $\hat{\varrho}$, find a Hamiltonian $\hat{\mathcal{H}}$ and inverse temperature $\beta=1/T$ so that

$$\hat{\varrho}=\frac{1}{Z}e^{-\beta\hat{\mathcal{H}}}, \tag{28}$$

where $Z=\mathrm{tr}[\exp(-\beta\hat{\mathcal{H}})]$. In other words, we are looking for a canonically populated system $\hat{\mathcal{H}}$ that reproduces (for a certain temperature T) our statistical ensemble $\hat{\varrho}$. For a parameter-dependent density matrix $\hat{\varrho}^\alpha(\lambda)$ from Eq. (10) we have the effective Hamiltonian

$$\hat{\mathcal{H}}^\alpha(\lambda)=\sum_{p=1}^{n}|\phi_p^\alpha(\lambda)\rangle\epsilon_p^\alpha(\lambda)\langle\phi_p^\alpha(\lambda)|, \tag{29}$$

where ''energies'' $\epsilon_p^\alpha(\lambda)$ are to be calculated along with $\beta^\alpha(\lambda)$ so that Eq. (28) be satisfied. It should be remembered that the results of this procedure depend, in general, on the value of λ and the initial state α. For the sake of simplicity, however, we will sometimes omit the explicit mentioning of this dependence in the following derivations.

The condition (28) gives us n equations. Since the number of variables to be found is $n+1$ (energies plus the temperature), the solution cannot be unique. Indeed, the scaling transformation $\beta\to\beta/c$, $\epsilon_p\to c\epsilon_p$ (where c is an arbitrary constant) certainly does not change the validity of Eq. (28). One can therefore impose an additional constraint. It is physically plausible to set the energy average of the equivalent canonical ensemble to the mean energy of the term E^α in the range of the parameter change,

$$\langle\epsilon\rangle=\int d[\delta\lambda]p(\delta\lambda)E^\alpha(\lambda). \tag{30}$$

Because of the normalization of the density matrix, we have an additional freedom of fixing one more physical parameter. This can be used in order to prescribe the energy dispersion of the canonical ensemble in the following way:

$$\begin{aligned}\langle\Delta^2\epsilon\rangle&\equiv\langle\epsilon^2\rangle-\langle\epsilon\rangle^2\\&=\int d[\delta\lambda]p(\delta\lambda)[E^\alpha(\lambda)]^2\\&\quad-\left[\int d[\delta\lambda]p(\delta\lambda)E^\alpha(\lambda)\right]^2.\end{aligned} \tag{31}$$

This procedure leads to the following set of equations:

$$\rho_p=\frac{1}{Z}e^{-\beta\epsilon_p}\quad\text{for}\quad p=1\ldots n, \tag{32}$$

$$S=\beta\langle\epsilon\rangle+\ln Z, \tag{33}$$

$$S'-S^2=\beta^2\langle\Delta^2\epsilon\rangle, \tag{34}$$

where

$$S' = \sum_{p=1}^{n} \rho_p (\ln \rho_p)^2 \tag{35}$$

is fixed, like S, by the initial density matrix. The set (32)–(34) can be solved from the bottom: given a prescribed value of the energy dispersion, Eq. (34) yields the inverse temperature β. It enters, along with the given energy average, Eq. (33), which then yields the partition sum Z. This, together with β from the previous step, enables one to determine individual energies $\{\epsilon_p\}$ from the equations under Eq. (32).

It is well known that in the canonical ensemble the energy fluctuation is proportional to squared temperature through a constant C that can be identified with the specific heat of the system: $\langle \Delta^2 \epsilon \rangle = CT^2$. With the aid of Eq. (34), we can easily determine the specific heat of our thermal equivalent:

$$C = S' - S^2 = -\sum_{p=1}^{n} \left[\rho_p \ln \rho_p \left(\sum_{p'=1}^{n} \rho_{p'} \ln \rho_{p'} - \ln \rho_p \right) \right]. \tag{36}$$

The quantity on the right-hand side measures the variability of the set of the pointer basis occupancies $\{\rho_p\}_{p=1}^n$: it is zero for the uniform or Kronecker delta forms of the probability distribution and increases with the increasing spread of probabilities within the interval $[0,1]$. For our goals, relative temperature in units of the rms energy, $T_{\rm rel} = T/\sqrt{\langle \Delta^2 \epsilon \rangle} = 1/\sqrt{C}$, might be more useful than $T = 1/\beta$ itself: while canonical temperature $T^\alpha(\lambda)$ depends on the behavior of $E^\alpha(\lambda)$, relative temperature $T^\alpha_{\rm rel}(\lambda)$ results solely from the mixing properties of the model Hamiltonian and therefore appears more universal. We thus deal only with $C = 1/T^2_{\rm rel}$ in the following. Note that although the temperature of the thermal equivalent could be at first expected to coincide with the level-density temperature $T_{\rm LD}$, which also implicitly depends on the mixing, the results given below do not agree with this expectation.

The question of typical values of the specific heat in Eq. (36) can be addressed by randomly generating the sets of pointer basis occupancies $\{\rho_p\}_{p=1}^n$ uniformly distributed on the hypersurface $\Sigma_p \rho_p = 1$ in n-dimensional space, and accumulating the distribution of $S' - S^2$. For $n \to \infty$, the result can be obtained analytically. In this limit, individual probabilities $\rho_p = a_p^2$ become independent random numbers with the Porter-Thomas distribution [28], i.e., with the Gaussian density

$$w_n(a_p) = \sqrt{\frac{n}{2\pi}} e^{-n a_p^2/2} \tag{37}$$

of the amplitudes a_p. The asymptotic form of the distribution in question is the δ function located at

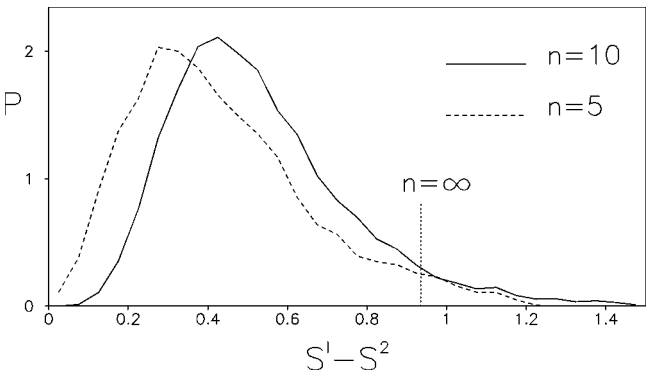

FIG. 6. The distribution of the heat capacity in Eq. (36) with the probabilities ρ_p randomly generated for dimensions $n=5$ and 10. Also indicated is the asymptotic value (38).

$$[S' - S^2]_\infty = n \int_{-\infty}^{+\infty} da\, w_n(a) a^2 (\ln a^2)^2 - \left[n \int_{-\infty}^{+\infty} da\, w_n(a) a^2 \ln a^2 \right]^2 = \frac{\pi^2}{2} - 4. \tag{38}$$

However, the convergence to this limit is rather slow in reality. Figure 6 shows the distribution of $S' - S^2$ for $n=5$ and 10 obtained from 10^4 generated sets $\{\rho_p\}_{p=1}^n$. In both cases, the peak is still wide and located well below the limit (38). The sensitivity of the distribution in Fig. 6 to the dimension implies that the expectation range of the specific heat depends on the number of states involved in the random mixing.

In Fig. 7, we present the specific heat (36) C^α corresponding to the first, fourth and thirtieth eigenstate with $L=0$ of the model Hamiltonian (2) (again $N=30$) as a function of λ. It is clear that the regions where the values of C^α significantly increase coincide with the regions of enhanced S in respective Figs. 2–4. Typical maxima of the specific heat in Fig. 7 do not reach the asymptotic value (38) but agree more or less with lower-dimension expectation values from Fig. 6. It means that an effective dimension $n_{\rm eff}$ given by the number of essentially nonzero eigenvalues ρ_p is much less than the total number of $L=0$ eigenstates ($n=91$). This agrees with the notion discussed in Ref. [6] on the basis of the perturbative calculations: roughly speaking, the number of principal components admixed in the pointer basis is determined by the characteristic order of perturbation theory (number of admixed exciton classes in Fermi systems). One can also notice an apparent correspondence between single peaks in the plots of S (Figs. 2–4) and couples of peaks (''twin peaks'') in the respective plots of C (Fig. 7). This suggests the following scenario for the mixing in a vicinity of avoided crossings. At first, as the two or more levels become closer, the distribution of ρ_p deviates from the Kronecker delta form so that both S and C increase. As one proceeds towards the avoided crossing point, roughly a uniform population $\rho_p \approx 1/n_{\rm eff}$ of involved states is developed,

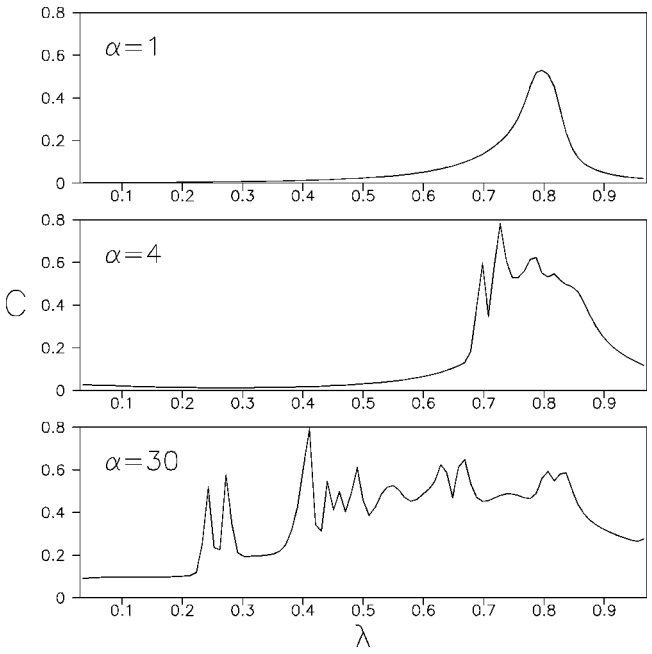

FIG. 7. The specific heat, Eq. (36), derived from the thermal equivalent of the density matrix (8) as a function of λ. The panels from top to bottom correspond to the ensembles associated with the first, fourth, and thirtieth eigenstate of Eq. (2) with $L=0$ and $N=30$.

which leads to a further increase of *S*, but at the same time to the observed decrease of *C* [see the explanation below Eq. (36)]. In some cases the peaks in *C* do not split—see, e.g., the upper panel of Fig. 7. This means that the mixing does not always lead to the quasiuniform population. We checked that the splitting also depends on the range of the parameter fluctuations; for example, for $\sigma=0.05$, the $\alpha=1$ maximum in *C* is already doubled.

Entropy *S* and specific heat *C* for the ground state have sharp maxima at $\lambda=0.8$, see upper panels in Figs. 2 and 7. Although these effects could be expected from earlier arguments based on the local increase of mixing around that point, they provide a physical insight into the related quantum critical phenomenon [17]. When dealing with the abrupt SU(3)→U(5) change of the ground-state structure in the IBM, the term ‘‘ phase transition’’ is usually put in parentheses or modified [18] to avoid a direct identification with thermodynamic phase transitions [22]. The same holds true for similar findings in fermionic models [29–31]. Now we found a way how such effects can be translated into a truly thermodynamic language—into properties of the thermal equivalent. Of course, we still deal with a finite system where no change is really discontinuous. It is natural to expect that for infinite boson numbers both *S* and *C* become singular at the critical point.

V. CONCLUSIONS

We studied some features of a parameter-dependent random Hamiltonian $\hat{H}(\lambda+\delta\lambda)$ with the parametric dependence carried by the mean value λ and randomness induced by the fluctuation $\delta\lambda$. In particular, we used the IBM-1 describing a finite bosonic system, where λ controls transitions between two incompatible dynamical symmetries, SU(3) and U(5), and fluctuations are mediated by a stochastic strength of an incompatible perturbation, see Eq. (5). Since individual eigenstates of the unperturbed Hamiltonian (2) turn into density matrices (8) in the presence of fluctuations, it is possible to naturally introduce quantities known from statistical physics like entropy, temperature etc. We developed a simple method that allows one to supply a given statistical ensemble by its ‘‘ thermal equivalent,’’ keeping both the energy average and dispersion fixed, see Eqs. (32)–(34).

For the whole range of λ covering the crossover region between the limiting dynamic symmetries, we numerically evaluated (for selected states) coherent (von Neumann) entropy and incoherent (information) entropy in the local basis (15). In the regime of small fluctuations they fulfill the simple perturbative relation (25). These entropies were found to be sensitive to the mixing induced by avoided crossings of levels in the λ-dependent spectrum (compare Figs. 1 and 2–4). In particular, the multiple avoided crossing at $\lambda\approx0.8$ was shown to be substantial (Figs. 2 and 3). We also studied—with the aid of overlap entropy (14)—the relation of the pointer basis (density-matrix eigenbasis at a given λ) to other relevant bases. The overlap of the pointer basis with the SU(3) basis is more or less random within the whole parameter range, while the overlaps with the local and U(5) bases strongly increase approaching the U(5) limit (Figs. 2–4). Moreover, for the low-lying states, the U(5) basis itself seems to be an ‘‘ attractor’’ for the pointer basis above $\lambda\approx0.8$ (Figs. 2 and 3). This feature may invoke a similar expectation of a strong dependence on parameters also for a more realistic, environment-induced selection mechanism of the pointer basis.

Along with entropies, we calculated the λ-dependence of the specific heat (36) attributed to the given density matrix (8) via its thermal equivalent. It is determined as the proportionality constant between the energy dispersion and the squared temperature of the thermal equivalent. We showed that the specific heat also reflects the $\delta\lambda$-induced mixing of eigenfunctions, but in a way different from coherent entropy. It typically develops single and double peaks near avoided crossings (compare Figs. 1 and 7). An expected range of values of the specific heat in case of a random mixing was derived, see Fig. 6.

An important focus of our interest was the search for new dynamical signatures of the ‘‘quantum phase transition’’ between the SU(3) and U(5) symmetries, described so far only on the level of energy eigenfunctions. We have discussed several new results related to this point. (i) The ridge in the plot of thermodynamic (based on the level density) temperature at $\lambda=0.8$, see Fig. 5, is directly connected to the specific level dynamics shown in Fig. 1. (ii) The attraction of the pointer basis associated with low-lying states towards the U(5) basis can also be considered as a phase-transitional signature. Although this effect is not clearly understood yet, it reminds of a similar tendency of individual low-energy eigenfunctions. (iii) Ground-state entropy with a sharp peak (Fig. 2, top) at the critical point and (iv) the specific heat

with a similar behavior (Fig. 7, top) are the signatures presumably related to standard thermodynamics of phase transitions.

In all cases we look at the critical parameter region through the response of individual eigenstates; this response is smeared for states higher in energy. On the other hand, a surprising and nontrivial result is the attraction of the pointer basis towards the U(5) dynamical symmetry basis for low-energy states in the region above the critical parameter value. We believe that these examples illustrate the potential complexity of situations that one can deal with when studying the decoherence process. In particular, interesting questions are raised by the possibility of using different entropylike and temperaturelike quantities for the description of the randomization of a mesoscopic system by an external noise. The interrelation between chaos, thermalization, and decoherence is a promising subject for future studies.

ACKNOWLEDGMENTS

This work was supported by the NSF Grant Nos. 96-05207 and 00-70911, and partly by the GAČR Grant No. 202/99/1718. P.C. and V.V.S. thank the National Superconducting Cyclotron Laboratory for its hospitality and excellent working conditions.

[1] R. Kubo, M. Toda, and N. Hashitsume, *Statistical Physics II Nonequilibrium Statistical Mechanics*, Springer Series in Solid State Sciences Vol. 31 (Springer-Verlag, Berlin, 1983).
[2] T.A. Brody *et al.*, Rev. Mod. Phys. **53**, 385 (1981).
[3] S.S.M. Wong, *Nuclear Statistical Spectroscopy* (Oxford University Press, New York, 1986).
[4] V.V. Flambaum and F.M. Izrailev, Phys. Rev. E **56**, 5144 (1997).
[5] C.W. Johnson, G.F. Bertsch, and D.J. Dean, Phys. Rev. Lett. **80**, 2749 (1998).
[6] V.V. Sokolov, B.A. Brown, and V. Zelevinsky, Phys. Rev. E **58**, 56 (1998).
[7] R. Bijker and A. Frank, Phys. Rev. Lett. **84**, 420 (2000).
[8] D. Mulhall, A. Volya, and V. Zelevinsky, Phys. Rev. Lett. **85**, 4016 (2000).
[9] T. Guhr, A. Müller-Groeling, and H.A. Weidenmüller, Phys. Rep. **299**, 189 (1998).
[10] W.H. Zurek, Phys. Rev. D **26**, 1862 (1982).
[11] W.H. Zurek, S. Habib, and J.P. Paz, Phys. Rev. Lett. **70**, 1187 (1993).
[12] J.P. Paz and W.H. Zurek, Phys. Rev. Lett. **82**, 5181 (1999).
[13] M. Srednicki, Phys. Rev. E **50**, 888 (1994).
[14] M. Horoi, V. Zelevinsky, and B.A. Brown, Phys. Rev. Lett. **74**, 5194 (1995).
[15] V. Zelevinsky, B.A. Brown, N. Frazier, and M. Horoi, Phys. Rep. **276**, 85 (1996).
[16] V. Zelevinsky, Annu. Rev. Nucl. Part. Sci. **46**, 237 (1996).
[17] P. Cejnar and J. Jolie, Phys. Rev. E **61**, 6237 (2000).
[18] F. Iachello and A. Arima, *The Interacting Boson Model* (Cambridge University Press, Cambridge, England, 1987).
[19] A. Frank and P. Van Isacker, *Algebraic Methods in Molecular and Nuclear Structure Physics* (Wiley, New York, 1994).
[20] A.E. Dieperink, O. Scholten, and F. Iachello, Phys. Rev. Lett. **44**, 1747 (1980).
[21] D.H. Feng, R. Gilmore, and S.R. Deans, Phys. Rev. C **23**, 1254 (1981).
[22] L.D. Landau and E.M. Lifshitz, *Statistical Physics* (Pergamon Press, Oxford, 1958).
[23] V. Zelevinsky, M. Horoi, and B.A. Brown, Phys. Lett. B **350**, 141 (1995).
[24] F.M. Izrailev, Phys. Lett. A **134**, 13 (1988).
[25] P. Cejnar and J. Jolie, Phys. Rev. E **58**, 387 (1998).
[26] D. Kusnezov and D. Mitchell, Phys. Rev. C **54**, 147 (1996).
[27] D. Kusnezov, B.A. Brown, and V. Zelevinsky, Phys. Lett. B **385**, 5 (1996).
[28] H. Feshbach, *Theoretical Nuclear Physics Nuclear Reactions* (Wiley, New York, 1992), p. 286.
[29] D.J. Thouless, Nucl. Phys. **22**, 78 (1961).
[30] E.D. Davis and W.D. Heiss, J. Phys. G **12**, 805 (1986).
[31] W.D. Heiss and A.L. Sannino, Phys. Rev. A **43**, 4159 (1991).